Journal of Chromatography A, 662 (1994) 1–12
Elsevier Science B.V., Amsterdam

CHROM. 25 717

Computer simulation study of multi-detector size-exclusion chromatography of branched molecular mass distributions

Christian Jackson

E.I. du Pont de Nemours and Company, Central Research and Development, Experimental Station, P.O. Box 80228, Wilmington, DE 19880-0228 (USA)

(First received August 10th, 1993; revised manuscript received October 5th, 1993)

ABSTRACT

Size-exclusion chromatography (SEC) provides a rapid method for determining molecular mass distributions relative to standard calibration materials. If light-scattering and viscosity detectors are used independent measurements of molecular mass and size can be obtained directly, and these can be used to estimate the distribution of branching across the molecular mass distribution. In order to study the effect of branching on the detector signals and the calculated results a computer simulation of the multiple detector SEC analysis of randomly branched polymers was developed. The model is described and results for different amounts of branching, different extents of reaction, and different models of the hydrodynamic size are discussed.

INTRODUCTION

The integration of molecular mass-sensitive detectors with size-exclusion chromatography (SEC) increases the amount of information that can be determined in the analysis. Measurement of the light-scattering intensity and the sample concentration enables the molecular mass distribution (MMD) to be determined directly without column calibration. These data can be combined with the universal calibration curve describing hydrodynamic size as a function of elution volume, to determine the intrinsic viscosity at each elution volume element. Measurement of the specific viscosity, using a continuous viscometer, and sample concentration enables the intrinsic viscosity distribution to be determined directly without column calibration. Universal calibration can then be used to calculate the MMD [1–4].

If light-scattering (LS) and viscosity (Visc) detectors are used, both molecular mass and intrinsic viscosity distributions can be measured directly. This method is particularly suited to the characterization of polymer conformation and branching because the relationship between molecular mass and molecular size, determined from the intrinsic viscosity, is measured across the MMD. Changes in this relationship can be related to the amount of branching or change in conformation [5,6].

Unfortunately, because both branching and molecular mass affect the molecular hydrodynamic size, the one-dimensional size-exclusion separation no longer gives full resolution of the MMD. Instead, only a partial resolution is possible, with the possibility that branched polymer molecules may be unresolved from linear molecules with a different molecular mass, but the same hydrodynamic size.

In addition to the problem of SEC resolution, the LS detector and the viscometer respond differently to branching. In general branching will increase molecular mass and thus the intensity of scattered light; however, the intrinsic viscosity of a branched polymer is less than that of

0021-9673/94/$07.00
SSDI 0021-9673(93)E1177-2

its linear analogue, and so the viscometer response is decreased relative to that for a linear molecule.

In order to gain a better understanding of how these factors affect the experiment and the possible errors involved in the calculated results we developed a computer simulation of the SEC–Visc–LS separation and analysis of a randomly branched condensation polymer.

METHODOLOGY

Molecular mass distribution model

The model MMD used is that developed by Stockmayer and also by Flory [7–9] using a mean-field approach. This model assumes equal intrinsic reactivities and excludes intramolecular reaction between finite species, and more sophisticated treatments have been developed. However, it provides a useful approximation, especially for low degrees of branching. In dilute solution measurements of branching we are interested in comparing the properties of the branched molecule to those of the linear molecule. As the Flory–Stockmayer model reduces to the most probable distribution for linear polymerizations both linear and branched MMDs can be simulated. This makes it preferable to more recent percolation models of branched MMDs [10,11]. The methods for calculating the experimental detector responses follow those developed previously for linear MMDs [12,13].

The model MMD used is for the random condensation of bifunctional monomers with a small amount of trifunctional monomers. This results in structures such as the one shown in Fig. 1.

If the molecular mass of each monomer is considered equal, then the mass fraction of molecules with n trifunctional monomers and l bifunctional monomers is given by

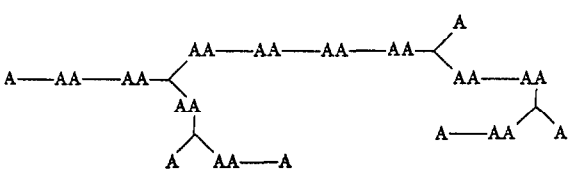

Fig. 1. Typical molecular structure produced by the polymerization model.

$$w_{n,l} = \frac{2(1-p)^2}{p(3-\rho)} \cdot \xi^n \eta^l (n+l)\omega_{n,l} \quad (1)$$

where p is the extent of the reaction, and ρ is the ratio of A groups belonging to branch units to the total number of A groups.

$$\rho = \frac{3N_0}{3N_0 + 2L_0} \quad (2)$$

N_0 and L_0 are the numbers of trifunctional and bifunctional monomers, respectively, and

$$\xi = p\rho(1-p) \quad (3)$$

$$\eta = (1-\rho)p \quad (4)$$

$$\omega_{n,l} = \frac{3(l+2n)!}{l!n!(n+2)!} \quad (5)$$

The monomer molecular mass was set arbitrarily at 100 g/mol. Mass fractions for up to 50 branch points per molecule ($n = 50$) were calculated for each MMD simulated.

If there are no trifunctional monomers eqn. 1 reduces to the equation for the most probable distribution.

$$w_l = (1-p)^2 l p^{(l-1)} \quad (6)$$

Size-exclusion chromatography model

SEC separates the sample by hydrodynamic volume rather than molecular mass, so that the MMD in eqn. 1 needs to be transformed into a hydrodynamic volume distribution [14].

Branching changes the relationship between hydrodynamic volume and molecular mass because a branched molecule is smaller than a linear molecule of the same molecular mass. This decrease in size is described by the branching index, g, which is the ratio of the mean square radius of gyration $\langle R_G \rangle^2$ of the branched molecule to that of the linear molecule with the same molecular mass (M) [15,16],

$$g = \left[\frac{\langle R_G \rangle^2_{\text{branched}}}{\langle R_G \rangle^2_{\text{linear}}} \right]_M \quad (7)$$

This ratio can be directly related to the number of branch points if the radius of gyration is measured under θ conditions, where the effect of excluded volume on the radius of gyration is apparently cancelled by Van der Waals attractions between segments of the chain. For exam-

ple, for a randomly branched polydisperse polymer with trifunctional branch points the weight-average value of g is given by

$$g_w = \frac{3}{n_w}\left(\frac{2+n_w}{n_w}\right)^{1/2} \cdot \ln\left(\frac{(2+n_w)^{1/2}+n_w)^{1/2}}{(2+n_w)^{1/2}-n_w^{1/2}} - 1\right) \quad (8)$$

where n_w is the number of trifunctional branch points per weight-average molecule.

The decrease in the hydrodynamic volume is described by g' which is defined as the decrease in intrinsic viscosity $[\eta]$ at a given molecular mass due to branching

$$g' = \left(\frac{[\eta]_{branched}}{[\eta]_{linear}}\right)_M \quad (9)$$

This is expected to be proportional to the decrease in the radius of gyration

$$g' = g^{\epsilon} \quad (10)$$

In this study it is assumed that the hydrodynamic radius remains proportional to the radius of gyration for branched polymers and so ϵ is set equal to 3/2. Experimentally its value is found to vary from 1/2 to 3/2. The effect of this variation in ϵ on the results is discussed below [17,18].

The SEC experiment is carried out using a thermodynamically good solvent and so it is assumed also that the radii of gyration of the branched and linear polymers have the same expansion factors. This assumes that the relationship between g and the number of branch points is insensitive to solvent quality and that the results based on eqns. 7 and 8 are still valid [19].

For the linear molecules the molecular mass is related to the column elution volume (V) by a calibration curve of the form

$$M_{n=0} = D_1 e^{-D_2 V} \quad (11)$$

where D_1 and D_2 describe the calibration curve for a given column set.

For branched molecules the calibration curve is shifted to larger elution volumes due to the reduction in size of the molecule. This shift is calculated from the equivalence of hydrodynamic sizes at each elution volume and by describing the relationship between intrinsic viscosity and molecular mass by the Mark–Houwink equation. If n is the number of branch points then from eqn. 9, the Mark–Houwink relationship for each n-mer, where an n-mer is the set of molecules with n trifunctional monomers and any number of bifunctional monomers, is given by

$$[\eta]_n = g_n' K M^a \quad (12)$$

where K and a are the Mark–Houwink coefficients for the linear polymer in the solvent. These are set to $1.2 \cdot 10^{-4}$ dl mol g^{-2} and 0.725, respectively, which are typical values for a polymer in a good solvent. The viscometric branching factor g_n' is calculated from eqns. 8 and 10.

The calibration curve for each n-mer can then be written as

$$M_n = [g']^{-1/(a+1)} D_1 e^{-D_2 V} \quad (13)$$

Eqn. 13 can be used to calculate the elution volume of each mass fraction in eqn. 1.

In SEC the mass fraction is measured as a function of the logarithm of molecular mass, so the mass fraction in eqn. 1 is modified to

$$w_{n,i}' = \frac{dM}{d \ln M} w_{n,i} \quad (14)$$

Light-scattering model

In the SEC–LS measurement the polymer can be considered to be at infinite dilution, in which case the intensity of scattered light at zero degrees with respect to the incident beam is directly proportional to the weight-average molecular mass of the polymer at each elution volume

$$I_{\theta=0} = K^* M_w w' \quad (15)$$

where K^* is an optical constant for the scattering system and w' is the mass fraction of all species at a given elution volume. All light scattering tracings shown correspond to the 0° scattering intensity.

Viscosity model

The specific viscosity of the eluting polymer is given by

$$\eta_{sp} = [\eta]_w w' \quad (16)$$

where the intrinsic viscosity of each species is

determined from eqn. 12. The sample is assumed to be at infinite dilution, and the intrinsic viscosity is the weight-average of the intrinsic viscosities of all the species present at a given elution volume.

RESULTS AND DISCUSSION

Results for individual n-mer distributions

The MMD of a branched polymer can be thought of as a set of individual MMDs of each n-mer, *i.e.*, the set of molecules containing n branch points. Fig. 2 shows typical refractometer tracings for fractions with $n = 0$, 1 and 2 branch points per molecule for an MMD with $p = 0.995$ and $\rho = 0.001$. Notice that with increasing number of branch points the mass fraction of n-mer decreases, the average molecular mass increases, and the elution volume decreases. The most highly branched material will be at the high end of the MMD, and the low end in this case is predominantly linear polymer. The molecular mass at each elution volume is also shown for the three fractions. At a given elution volume the n-mer with more branch points has a higher molecular mass than less branched molecules (eqn. 13).

Fig. 3 shows the Mark–Houwink plots for the three fractions. For a given molecular mass value, the intrinsic viscosity decreases with increasing number of branch points. However, according to the Zimm–Stockmayer theory the slope of the calibration curve is independent of the degree of branching for molecules with the same number of branch points but different molecular masses [15].

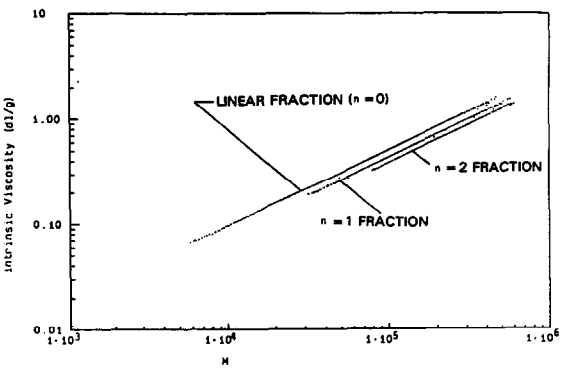

Fig. 3. Mark–Houwink plots of log M_w *vs.* log $[\eta]$ for the fractions of a branched MMD with 0, 1 and 2 branch points per molecule.

Fig. 4 shows simulated detector tracings for the complete distribution of n-mers for the distribution with $p = 0.995$ and $\rho = 0.001$. For this amount of branching the responses are very similar for each detector and there is little difference between the three peak shapes. As in the study of linear polymers, the LS intensity peak and the specific viscosity peak are both shifted to earlier elution volumes than the refractometer peak as a result of their molecular mass sensitivity. The viscosity peak is not shifted as

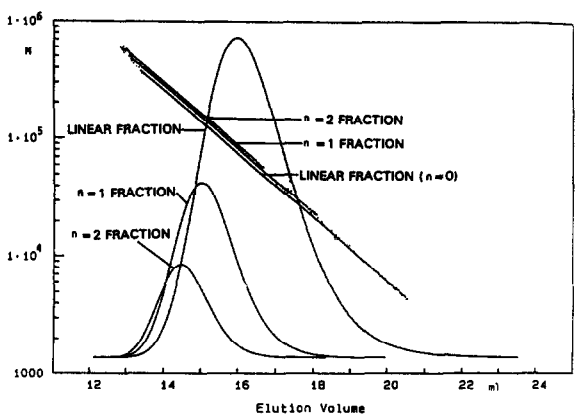

Fig. 2. Concentration detector response as a function of elution volume for fractions with 0, 1 and 2 branch points per molecule in a randomly branched MMD. The corresponding molecular mass calibration curves are also shown.

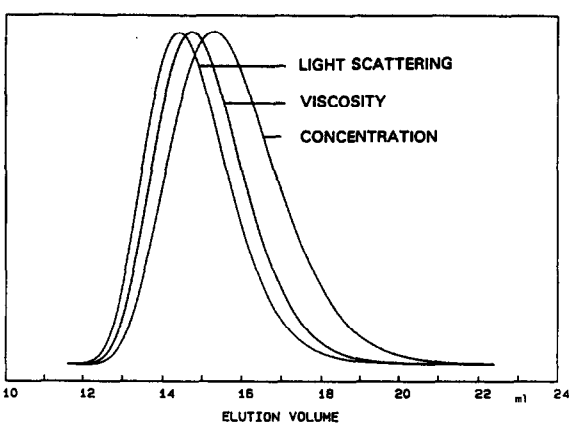

Fig. 4. Simulated tracings from the light-scattering, viscosity and refractive index detectors for a randomly branched MMD ($p = 0.995$, $\rho = 0.001$).

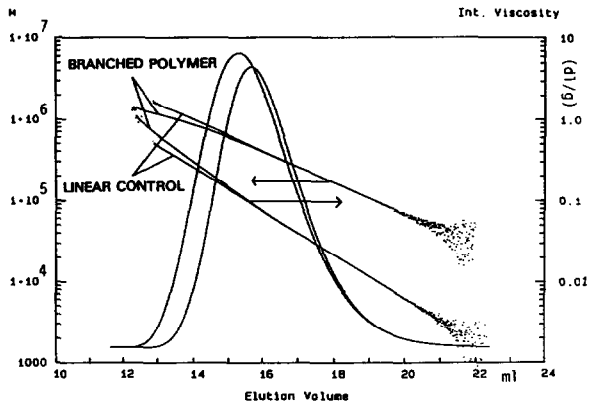

Fig. 5. Comparison of data from linear ($p = 0.995$) and branched ($p = 0.995$, $\rho = 0.001$) MMDs. The concentration detector responses are shown as well as the intrinsic viscosity and molecular mass at each elution volume.

much as the LS peak because it is less sensitive to molecular mass (eqn. 12). Branching causes slight differences in the relationship between the peak shapes and positions compared to those for the linear polymer which are discussed in detail below. However, in general the features for small amounts of branching are very similar to signals from linear MMDs. Fig. 5 shows calculated molecular masses and intrinsic viscosities as a function of elution volume for this distribution compared to a linear polymer at the same extent of reaction.

Fig. 6 shows the Mark–Houwink plot for the data. Although the slope for each fraction is a straight line the complete polymer gives a curved

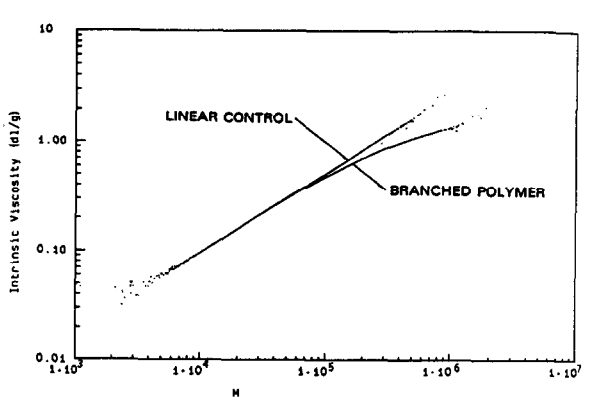

Fig. 6. Comparison of Mark–Houwink plots for the data from the linear and branched MMDs shown in Fig. 5.

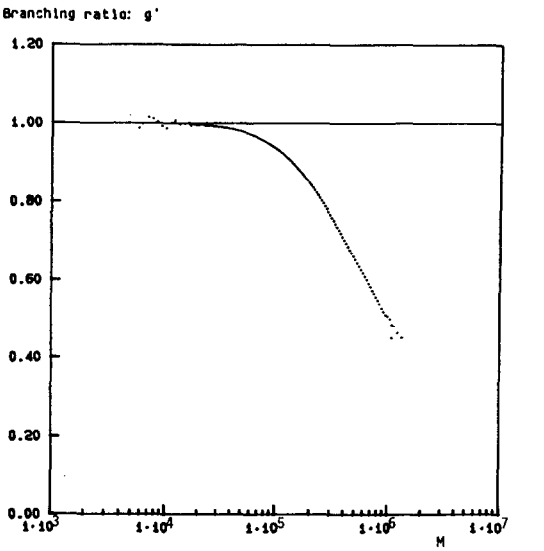

Fig. 7. Branching factor g' as a function of molecular mass for the branched polymer MMD shown in Figs. 3–5.

plot because different degrees of branching are not evenly distributed across the MMD. Fig. 7 shows the branching factor g' as a function of molecular mass. The value of the branching index is unity at the lowest molecular masses, reflecting the presence of predominantly linear polymer and rapidly decreases as molecular mass increases reflecting increased branching at the high end of the MMD.

Effect of extent of reaction

Six sets of data were generated at different extents of reaction ($p = 0.95$, 0.98, 0.99, 0.995, 0.9975 and 0.999) for a branched polymer with $\rho = 0.001$. Figs. 8, 9 and 10 show the refractometer, viscometer and light-scattering detector signals respectively, for the last five of these data sets. In each of the three figures the peak at the lowest elution volume corresponds to the greatest extent of reaction and highest molecular mass, while the peak at the highest elution volume is the lowest extent of reaction and molecular mass ($p = 0.98$). The refractometer tracings clearly show that as the reaction proceeds the MMD is broadened and increasingly skewed to the high-molecular-mass side of the distribution. The areas under the viscometer and LS tracings show the large increase in molecular

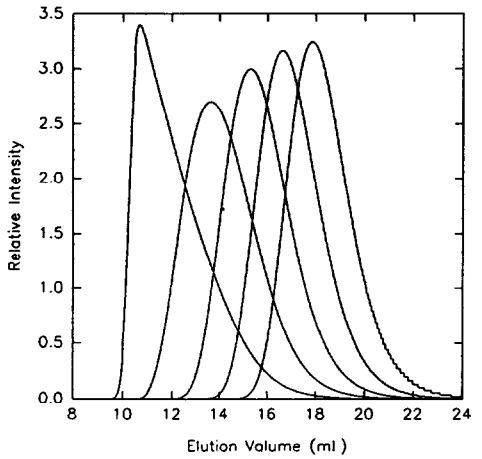

Fig. 8. Concentration detector tracings for branched MMDs at different extents of reaction for a branched polymer MMD with $\rho = 0.001$. From left to right the peaks correspond to $p = 0.999$, $p = 0.9975$, $p = 0.995$, $p = 0.990$ and $p = 0.980$.

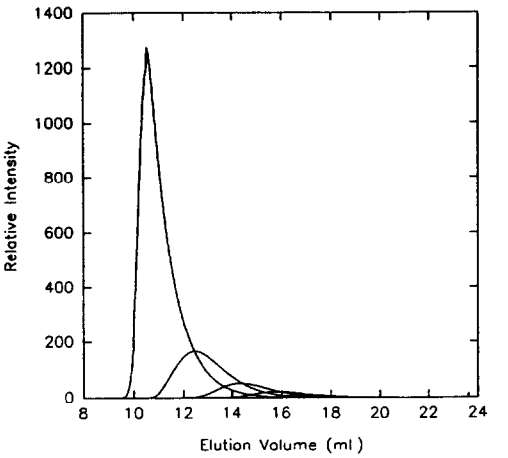

Fig. 10. Light-scattering detector tracings (0°) for branched MMDs at different extents of reaction for a branched polymer MMD with $\rho = 0.001$. From left to right the peaks correspond to $p = 0.999$, $p = 0.9975$, $p = 0.995$, $p = 0.990$ and $p = 0.980$.

mass and intrinsic viscosity of the polymer as the reaction proceeds. The viscosity signal increases less than the LS intensity because of the smaller intrinsic viscosity of branched molecules.

The highly skewed signals from the branched polymer at $p = 0.999$ is due to the proximity of the reaction to the gel point. Gelation occurs for this trifunctional case at a critical extent of reaction p_c given by

$$p_c = \frac{1}{1+\rho} \tag{17}$$

which for $\rho = 0.001$ is 0.999001, only slightly beyond $p = 0.999$. Since the polymer system is close to gelation, a significant mass fraction of the distribution is highly branched high-molecular-mass molecules concentrated at low elution volumes due to the poor resolution of SEC for such a mixture.

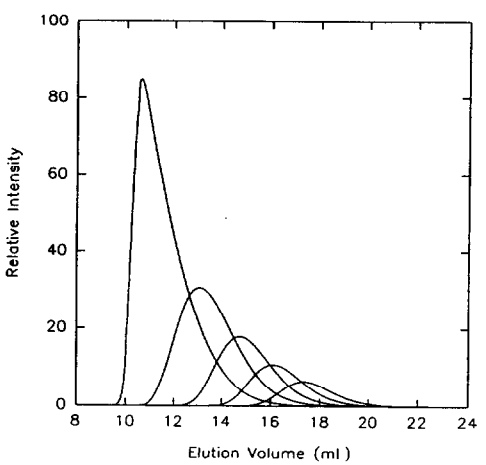

Fig. 9. Viscosity detector tracings for branched MMDs at different extents of reaction for a branched polymer MMD with $\rho = 0.001$. From left to right the peaks correspond to $p = 0.999$, $p = 0.9975$, $p = 0.995$, $p = 0.990$ and $p = 0.980$.

Fig. 11 shows the plots of the branching factor against the same molecular mass scale for the six extents of reaction listed above. As the reaction proceeds the degree of branching increases as does the molecular mass of the branched fractions. However, the slope of the curves at high molecular masses appears to be fairly constant. Table I lists the number-average, weight-average and z-average values of the branching factor for each value of the extent of reaction.

The number-average branching factor is defined as

$$g'_N = \frac{\sum_i N_i g'_i}{\sum_i N_i} \tag{18}$$

the mass-average branching factor is defined as

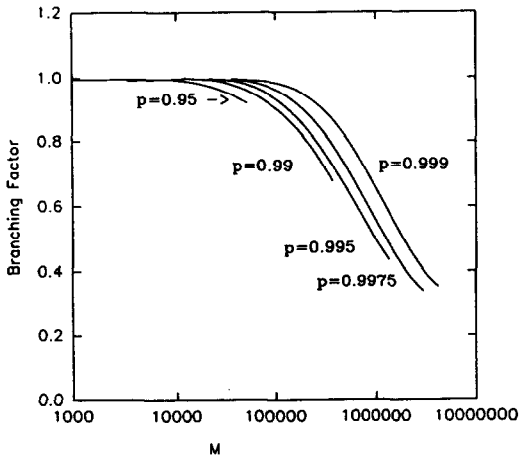

Fig. 11. Branching factor g' as a function of molecular mass for branched polymer MMD with different extents of reaction ($\rho = 0.001$).

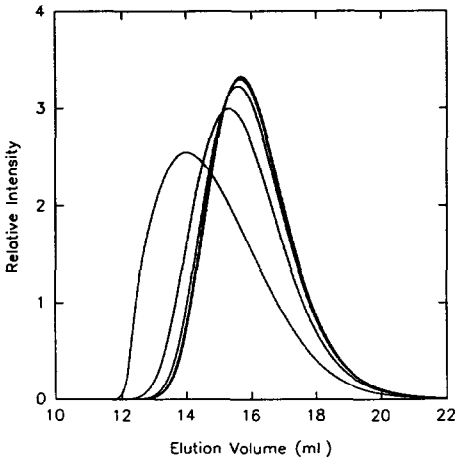

Fig. 12. Concentration detector tracings for branched MMDs with different fractions of branched monomer at extent of reaction $p = 0.995$. From left to right the peaks correspond to $\rho = 0.003$, $\rho = 0.001$, $\rho = 0.0003$, $\rho = 0.0001$ and $\rho = 0.00003$.

$$g'_w = \frac{\sum_i M_i N_i g'_i}{\sum_i M_i N_i} \quad (19)$$

and the z-average branching index is as

$$g'_z = \frac{\sum_i M_i^2 N_i g'_i}{\sum_i M_i^2 N_i} \quad (20)$$

where i is the number of each elution volume element and N_i is the number of molecules in each volume element calculated from

$$N_i = \frac{M_i}{c_i} \quad (21)$$

where c_i is the concentration of polymer at each volume element.

TABLE I

NUMBER; WEIGHT- AND Z-AVERAGE BRANCHING INDICES FOR MMDs AT DIFFERENT EXTENTS OF REACTION AND $\rho = 0.001$

p	g'_n	g_w'	g'_z
0.9500	0.995	0.991	0.985
0.9800	0.985	0.979	0.950
0.9900	0.978	0.955	0.919
0.9950	0.962	0.908	0.833
0.9975	0.934	0.800	0.645
0.9990	0.874	0.618	0.460

Effect of the fraction of branched monomers

A second set of data was generated for distributions at the same extent of reaction ($p = 0.995$) but with increasing amounts of branched monomer ($\rho = 0.00003$, 0.0001, 0.0003, 0.001 and 0.003). Figs. 12, 13 and 14 show the signals

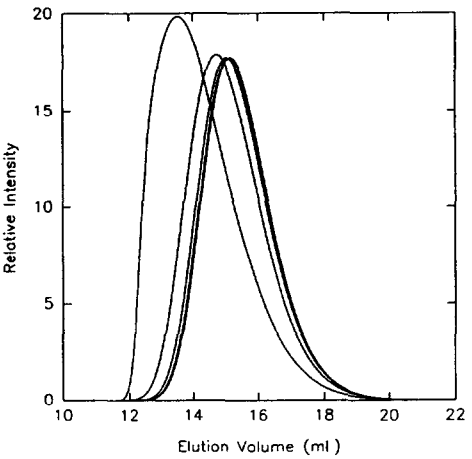

Fig. 13. Viscosity detector tracings for branched MMDs with different fractions of branched monomer at extent of reaction $p = 0.995$. From left to right the peaks correspond to $\rho = 0.003$, $\rho = 0.001$, $\rho = 0.0003$, $\rho = 0.0001$ and $\rho = 0.00003$.

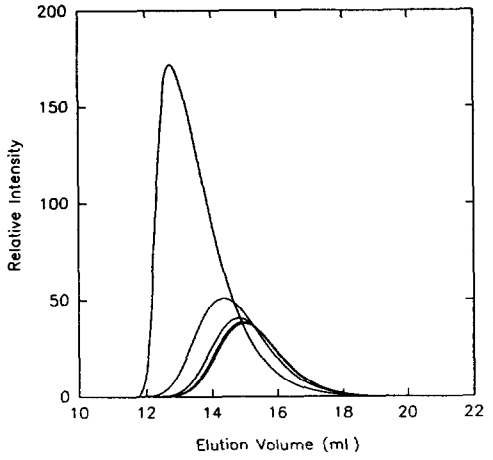

Fig. 14. Light-scattering detector tracings (0°) for branched MMDs with different fractions of branched monomer at extent of reaction $p = 0.995$. From left to right the peaks correspond to $\rho = 0.003$, $\rho = 0.001$, $\rho = 0.0003$, $\rho = 0.0001$ and $\rho = 0.00003$.

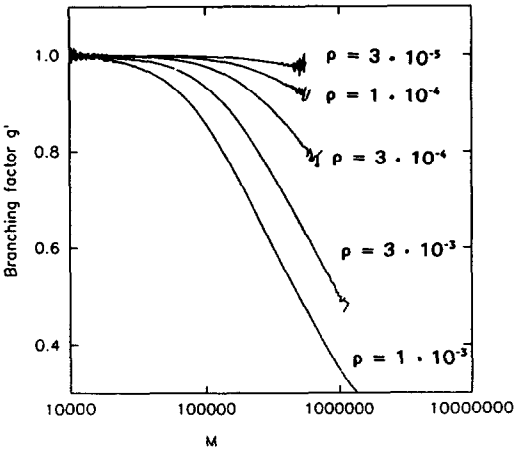

Fig. 15. Branching factor g' as a function of molecular mass for branched polymer MMD with different fractions of branched monomer ($p = 0.995$).

from the refractometer, viscometer and light scattering detector, respectively. In each figure the peak at the lowest elution volume is the one with the greatest amount of branched monomer and the peak at the highest elution volume the one with the least. The refractometer data show the broadening of the MMD and the increased skew, while the viscometer and LS detector data show the increase in intrinsic viscosity and molecular mass in addition to the broadening and skew of the distribution. The changes are qualitatively the same as for increasing extent of reaction.

Fig. 15 shows the plots of the branching factor against molecular mass. As the fraction of branched monomer increases the limiting slope at high molecular masses increases and moves to slightly higher molecular mass values. Table II lists the average g' values for each distribution.

Peak molecular masses

For the Flory–Schulz linear MMD the molecular mass at the elution fraction which gives the peak concentration signal is the weight-average molecular mass. The molecular mass of the elution fraction that gives the peak LS intensity is the z-average molecular mass and the peak viscometer signal is at an elution fraction with a molecular mass between weight- and z-averages, given by

$$M_{\text{Visc peak}} = (1 + a/2)M_{\text{w}} \tag{22}$$

where a is the exponent of the Mark–Houwink equation [7].

Fig. 16 shows the relationship between the concentration detector peak molecular mass and the weight-average molecular mass for both sets of data discussed above. The relationship between the molecular masses at the different detector peaks and the molecular mass moments of the distribution was found to be the same for the data from distributions at different extents of reaction and distributions with different fractions of branched monomer. A least-squares fit to the data gives

$$M_{\text{RI peak}} \approx M_{\text{w}}^{0.98} \tag{23}$$

TABLE II

NUMBER-, WEIGHT- AND z-AVERAGE BRANCHING INDICES FOR MMDs WITH DIFFERENT FRACTIONS OF BRANCHED MONOMERS AND $p = 0.995$

ρ	g'_{n}	g'_{w}	g'_{z}
0.00003	0.994	0.997	0.995
0.0001	0.996	0.991	0.983
0.0003	0.981	0.974	0.952
0.001	0.967	0.908	0.831
0.003	0.842	0.684	0.490

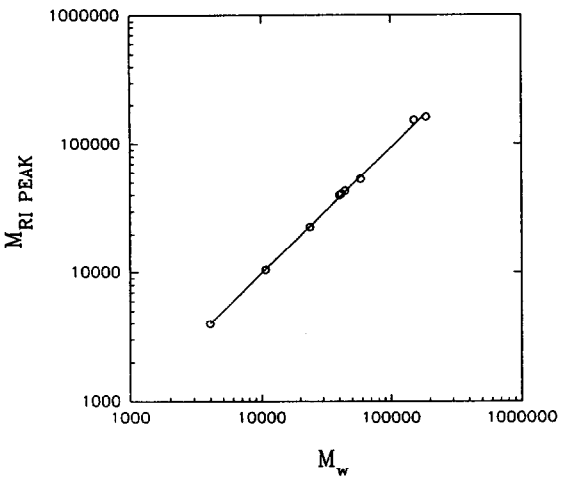

Fig. 16. Correlation of molecular mass at the maximum in concentration detector response with weight-average molecular mass.

The exponent is less than unity because as branching increases the MMD is increasingly dominated by low concentrations of high-molecular-mass, highly branched material. This shifts the weight-average molecular mass to higher values. Because of the relatively low concentration of these species the effect on the position of the maximum concentration signal is less.

Fig. 17 shows the relationship between the molecular mass at the LS intensity peak and the z-average molecular mass. The relationship between the two is

$$M_{\text{LS peak}} \approx M_z^{1.08} \tag{24}$$

The relationship with the weight-average molecular mass is

$$M_{\text{LS peak}} \approx M_w^{1.16} \tag{25}$$

The exponent is greater than unity because of the change in the shape of the distribution. There is a small amount of very-high-molecular-mass material which has a greater effect on the position of the LS intensity maximum than it does on the z-average molecular mass. For these branched MMDs the LS peak reflects a higher moment of the distribution than the z-average molecular mass. Another possible effect is due to molecular mass polydispersity at each elution volume. As branching increases the molecular mass at each elution volume will become increasingly polydisperse leading to an overestimate by light scattering of the number-average molecular mass at a given elution volume. This effect may be pronounced in the high-molecular-mass fraction of the distribution where the molecular mass at each elution volume will be overestimated, although it has little effect on calculations of the molecular mass moments. A manuscript discussing these effects in more detail is forthcoming.

These results are in qualitative agreement with recent studies on branched polymers close to the gel point although the experimental slopes are slightly higher [20–22]. The slope of the simulated data in eqn. 25 is less than the value of 2 predicted by the Flory–Stockmayer theory probably because the SEC model does not give a separation by molecular mass. The slope for the simulated data is expected to be sensitive to the model of the SEC separation of branched polymers used.

Fig. 18 shows the same data as Fig. 17 but for the molecular mass at the elution volume that gives the peak viscosity signal. In this case the situation is complicated because with increasing branching the intrinsic viscosity decreases relative to its value for a linear polymer and so the fit to the data curves slightly downwards at high molecular masses.

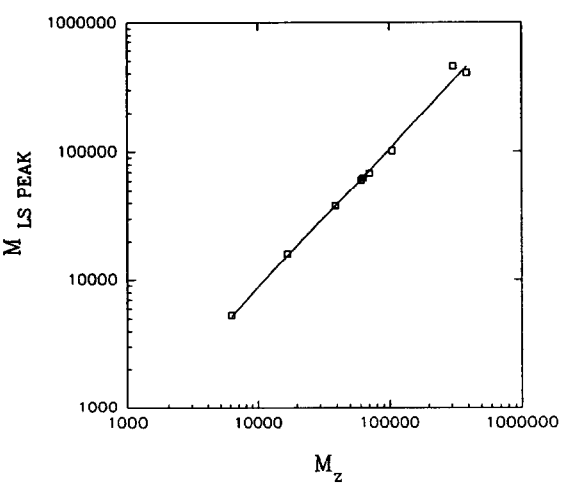

Fig. 17. Correlation of molecular mass at the maximum in light-scattering detector response with z-average molecular mass.

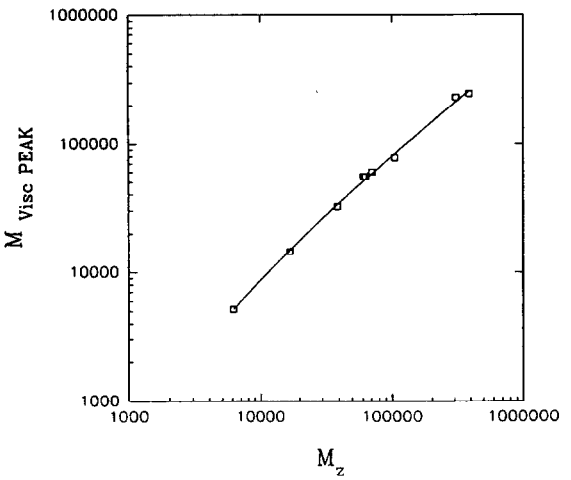

Fig. 18. Correlation of molecular mass at the maximum in viscosity detector response with z-average molecular mass.

Effect of SEC resolution on determination of molecular mass distribution

For a linear polymer there is a single-value relationship between a given hydrodynamic volume and molecular mass. For branched polymers this is no longer the case because a given elution volume from the chromatograph may contain molecules of different molecular masses but the same hydrodynamic radius. In this case we have imperfect resolution and the molecular mass polydispersity will be underestimated.

To study how large this loss of resolution is we calculated the true polydispersity as the MMD was generated, and compared this to the apparent polydispersity after transforming the MMD to the SEC MMD. Tables III and IV show these data for both variations in extent of reaction and variation in number of branch points. M_z/M_w is used as a measure of accuracy because it is the high-molecular-mass end of the distribution that is most sensitive to this loss of resolution.

TABLE III

TRUE AND MEASURED POLYDISPERSITIES, M_z/M_w, OF SAMPLE MMDs WITH $\rho = 0.001$

p ($\rho = 0.001$)	True M_z/M_w	SEC–LS M_z/M_w
0.9500	1.54	1.53
0.9800	1.58	1.57
0.9900	1.64	1.63
0.9950	1.79	1.78
0.9975	2.08	2.06
0.9990	1.72	1.71

TABLE IV

TRUE AND MEASURED POLYDISPERSITIES, M_z/M_w, OF SAMPLE MMDs WITH $p = 0.995$

ρ ($p = 0.995$)	True M_z/M_w	SEC–LS M_z/M_w
0.00003	1.51	1.51
0.0001	1.53	1.53
0.0003	1.59	1.58
0.001	1.79	1.78
0.003	2.04	2.03

The results show that there is very little loss of resolution and that the apparent MMD is very close to the true MMD. This can be understood by considering the elution profiles of different n-mers shown in Fig. 2. The MMDs for different n-mers only partially overlap because the average molecular mass increases greatly with increasing number of branch points. As a result a given elution volume does not contain a wide range of architecturally different molecules, but only a few whose molecular masses are very close. This means that the molecular mass polydispersity at most elution volumes is very small so that the average errors caused by measuring the loss of resolution are insignificant.

Effect of the relationship between the radius of gyration and the hydrodynamic radius

The previous data were generated assuming that the relationship between hydrodynamic radius and radius of gyration is independent of branching. Experimental and theoretical data indicate that the hydrodynamic radius may be less sensitive to branching than the radius of gyration, *i.e.*, for a given number of branch points the reduction in hydrodynamic radius relative to that of the linear polymer of the same molecular mass, is less than the reduction in the radius of gyration.

In order to show how this can affect the data

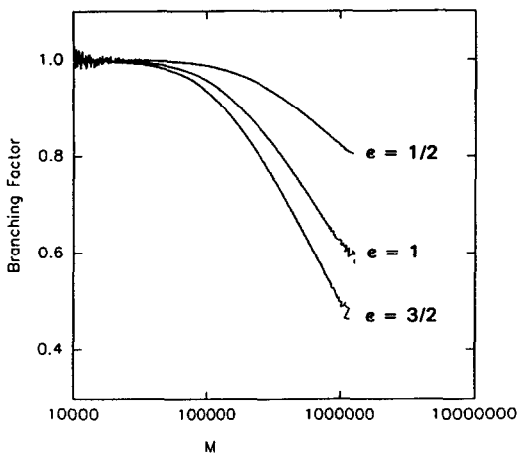

Fig. 19. Branching factor g' as a function of molecular mass for branched polymer MMD with different relationships between radius of gyration and hydrodynamic radius ($p = 0.995$, $\rho = 0.001$).

we generated two additional data sets where the exponent in eqn. 10 was set to 1 and 1/2. Data were generated for MMDs with $p = 0.995$ and $\rho = 0.001$. As the exponent decreases the sensitivity of the hydrodynamic volume to branching also decreases. This means that the chromatographic separation is less affected by branching, but that the size change caused by branching is more difficult to detect.

Fig. 19 shows branching factor plots for the data sets generated with $\epsilon = 1$, and 1/2 compared to 3/2. Table V shows the corresponding change in the average value of g'.

If Fig. 19 is compared with Fig. 15, it can be seen that the effect of changing ϵ is very similar to that of changing the number of branch points. For these reaction conditions changing ϵ from 3/2 to 1/2 has the same effect as decreasing the number of branch points by about an order of magnitude. It is clear that if g' is to be used to estimate the number of branch points in a polymer then ϵ must be determined first for the polymer–solvent system by careful measurements of the radius of gyration and intrinsic viscosity of samples with different amounts of branching. We are currently studying this problem using SEC combined with multi-angle laser-LS and viscosity detectors to measure both the radius of gyration and the intrinsic viscosity distributions of model branched polymers.

TABLE V

ϵ	g'_w
1/2	0.965
1	0.934
3/2	0.908

CONCLUSIONS

The simulation illustrates the expected behavior of the branching index and molecular mass for branched MMDs under different reaction conditions. Branching is greatest at the high-molecular-mass end of the MMD, at low molecular masses the polymer may be predominantly linear. Different averages of the branching index may be calculated, the z-average value is the most sensitive to branching. The relationship between the molecular masses at the peak of the LS tracing and the moments of distributions is in reasonable agreement with experiment. The loss of resolution in determining the MMD caused by branching is very small and is comparable to errors caused by signal noise. A significant problem with branching analysis by SEC with LS and viscosity detectors is determining the relationship between the decrease in intrinsic viscosity caused by branching and the number and functionality of those branches. Future work will look at the radius of gyration as a function of elution volume for the model and also the effect of gelation, and the SEC model used, on the different detector peak elution volumes and molecular masses.

ACKNOWLEDGEMENTS

I thank Howard Barth and the reviewers for numerous stimulating remarks.

REFERENCES

1 W.W. Yau, J.J. Kirkland and D.D. Bly, *Modern Size-Exclusion Chromatography*, Wiley, New York, 1979.
2 H.G. Barth and J.W. Mays (Editors), *Modern Methods of Polymer Characterization*, Wiley, New York, 1991.

3 A.R. Cooper (Editor), *Determination of Molecular Weight*, Wiley, New York, 1989.
4 J.J. Kirkland, S.W. Rementer and W.W. Yau, *J. Appl. Polym. Sci.*, 48 (1991) 39.
5 W.W. Yau, *Chemtracts*, 1 (1990) 1.
6 C. Jackson, H.G. Barth and W.W. Yau, in *Proc. Int. Gel Permeation Chromatography Symposium*, Waters Division of Millipore, Milford, MA, 1991.
7 P.J. Flory, *Principles of Polymer Chemistry*, Cornell University Press, Ithaca, NY, 1953, Ch. 8.
8 W.H. Stockmayer, *J. Chem. Phys.*, 11 (1943) 45.
9 W.H. Stockmayer, *J. Chem. Phys.*, 12 (1944) 125.
10 R.F.T. Stepto, in S.L. Aggarwal and S. Russo (Editors), *Comprehensive Polymer Science; First Supplement*, Pergamon Press, New York, 1992, Ch. 10.
11 D. Stauffer, *Introduction to Percolation Theory*, Taylor & Francis, New York, 1985.
12 C. Jackson and W.W. Yau, *J. Chromatogr.*, 645 (1993) 209.
13 C. Jackson and W.W. Yau, *Polym. Mater. Sci. Eng.*, 69 (1993) 212.
14 H. Benoit, Z. Grubisic, P. Rempp, D. Decker and J.G. Zilliox, *J. Chem. Phys.*, 63 (1963) 1507.
15 B.H. Zimm and W.H. Stockmayer, *J. Chem. Phys.*, 17 (1949) 1301.
16 H. Yamakawa, *Modern Theory of Polymer Solutions*, Academic Press, New York, 1971.
17 J. Roovers, in H.F. Mark (Editor), *Encyclopedia of Polymer Science and Engineering*, Wiley, New York, 2nd ed., 1989.
18 B.H. Zimm and R.W. Kilb, *J. Polym. Sci.*, 37 (1959) 19.
19 J.F. Douglas, J. Roovers and K.F. Freed, *Macromolecules*, 23 (1990) 4168.
20 F. Schosseler, H. Benoit, Z. Grubisic-Gallot, C. Strazielle and L. Leibler, *Macromolecules*, 22 (1989) 400.
21 E.V. Patton, J.A. Wesson, M. Rubinstein, J.C. Wilson and A.E. Oppenheimer, *Macromolecules*, 22 (1989) 1946.
22 J. Bauer, P. Lang, W. Burchard and M. Bauer, *Macromolecules*, 24 (1991) 2634.